JOURNAL OF APPLIED ELECTROCHEMISTRY 9 (1979) 629–634

Distribution profiles of antimony as a function of depth in corrosion films on a Pb-Sb alloy

F. ARIFUKU, H. YONEYAMA, H. TAMURA

Department of Applied Chemistry, Faculty of Engineering, Osaka University, Suita, Osaka, Japan

Received 11 November 1978

Distribution profiles of dissolved antimony in corrosion films on a Pb–Sb alloy were obtained by means of SIMS in the in-depth mode. The corrosion films were prepared by multi-triangular potential scans of the alloy in 5 M H_2SO_4. It was found that independent of the final polarization potential the dissolved antimony distributed in such a manner that there was a monotonically increasing trend in the content from the surface of the corrosion film to the lead alloy substratum.

1. Introduction

Lead–antimony alloys have been widely used as the grid material of lead–acid batteries. Antimony in the alloy is anodically dissolved from the grid even below the equilibrium $PbSO_4/PbO_2$ potential [1, 2]. Fortunately, however, the dissolved antimony improves the performance of the positive plate. In order to elucidate the benefical roles of antimony, it is helpful to obtain information on the distribution profiles for antimony within the film. The transference behaviour of dissolved antimony in electrolytes during charge–discharge cycles was studied by Dawson *et al.* [3, 4] by means of tracer techniques, but the distribution of antimony as a function of depth within the active material and the corrosion film has not yet been reported.

Several studies on secondary ion mass spectrometry in the in-depth mode [5–9] have shown that this technique is useful for analysing a specified element as a function of depth in the samples.

Therefore, our aim was to obtain distribution profiles of antimony as a function of depth in corrosion films on a lead–antimony alloy.

2. Experimental

2.1. *Preparation of samples*

Antimonial lead plates (4·92 wt% Sb) of a circular form (16 mm diameter, 2 mm thick) were used in the present study as the test electrodes. After mechanical polishing with a plane, the electrode was subjected to electropolishing in a mixed solution of CH_3COOH and $HClO_4$ (7:3) at 9 V for 10 min at room temperature. The electropolishing did not give a surface of metallic lustre but one covered with a black film. By wiping with wetted tissue paper, however, the black film was easily removed, and a brilliant surface of metallic lustre was obtained. The specimen was then mounted in a Teflon electrode holder, so that the surface exposed to the electrolyte was decreased to 0·95 cm^2. Before measurements were taken, the electrode was cathodically polarized at $-1{\cdot}2$ V for 30 min in 5 M H_2SO_4.

The electrolytic solution used in this study was 5 M H_2SO_4 which was prepared from reagent grade H_2SO_4 and doubly distilled water, and it was prepurified by electrolysis. A mercurous sulphate electrode in this solution was used as the reference electrode, and the potentials given in this paper are referred to this electrode. Nitrogen gas was bubbled through the solution for de-aeration and agitation of the solution, just prior to and sometimes during the measurements.

All the experiments were carried out at 25° C.

2.2. *Ion microprobe mass analysis*

The in-depth analysis was conducted by using an ion microanalyzer (Hitachi, model IMA-2). The techniques used here were analogous to those

0021–891X/79/050629–06 $02.60/0

reported by Evans *et al.* [7, 10] for the in-depth analysis of anodic oxide films on tantalum, except for the following conditions: acceleration voltage of the primary and secondary ion, 10 kV and ± 3 kV, respectively; primary Ar^+ beam density, 4×10^{-4} A cm^{-2} (0·5 μA/beam with the diameter of 0·40 mm); sample chamber, 10^{-7} torr pressure.

It is necessary in the in-depth analysis that the beam has a uniform intensity throughout the spot. To obtain such a condition, the primary beam was impinged onto the sample surface in an under-focussing condition [11], and the suitability of the condition was confirmed by the in-depth analysis of an anodic oxide film of tantalum formed up to 30 V by checking for a sharp change in the signal intensity of Ta^+ and O^- at the tantalum–oxide interface (see Fig. 6).

2.3. *Standard samples for in-depth analysis*

It is desirable to get information on the content of antimony in the corrosion film from secondary ion signal intensities of antimonial species. For this purpose, relationships between antimony contents and signal intensities must be obtained in advance by using standard samples containing known amounts of antimony. The preparation of the standard samples was follows: lead dioxide, and a mixture of lead sulphate and lead dioxide (80:20 wt%) were mixed with antimony oxides in various weight ratios, and the resulting mixtures were stirred in a wetted condition for 30 min, followed by drying under reduced pressure. Afterwards these were again mixed in an agate mortar for 30 min, and then pressed into a tablet form with 1·6 ton cm^{-2}.

In order to get a rough estimate of the thickness of the corrosion films from the sputtering time, the sputter rates were obtained for thin Pb, α-PbO_2 and β-PbO_2 films. These films were prepared on Pt by electrodeposition [12, 13].

3. Results and discussion

3.1. *Establishment of calibration curves*

Fig. 1 shows a negative secondary ion spectrum of an anodic corrosion film of the lead–antimony alloy. Though a variety of ionic fragments were produced by ion bombardment of the specimen, the highest intensities for antimony and lead species, of the secondary ion signals were obtained at $^{121}SbO_2^-$ and $^{208}PbO_2^-$ respectively. It was found that the relative sensitivity of secondary ions of antimony and lead were much higher for negative ions than for positive ions. From the results, signal profiles of SbO_2^- and PbO_2^- were chosen to obtain information on the distribution profiles of antimony in corrosion films of the antimonial lead.

In order to compensate for effects introduced by the variation of the primary ion intensity with time, it is desirable to use the ratio of signal intensity of SbO_2^- to that of PbO_2^-, I_{rel}, as a measure of the antimony content. This ratio was obtained for

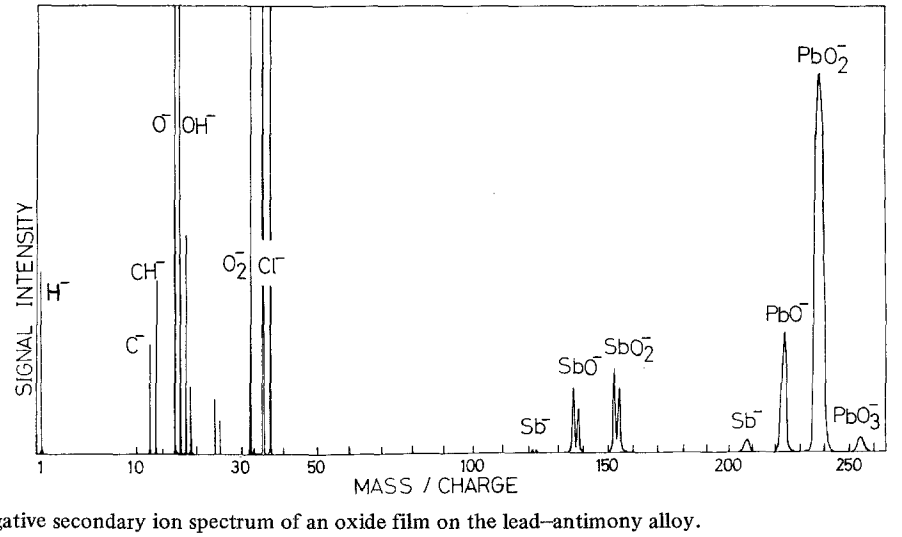

Fig. 1. Negative secondary ion spectrum of an oxide film on the lead–antimony alloy.

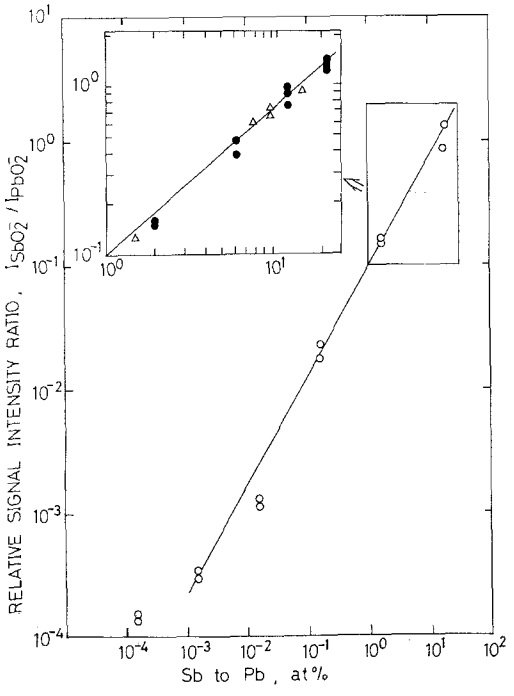

Fig. 2. Ratio of signal intensity of $^{121}SbO_2^-$ to that of $^{208}PbO_2^-$, I_{rel}, obtained on pressed disc samples containing a known amount of antimony, as a function of atomic ratio of Sb to Pb.

a variety of standard samples, and the results are given in Fig. 2. The open circles of Fig. 2 refer to samples compsed of PbO_2 and Sb_2O_3, and the triangular symbols to PbO_2 samples mixed with Sb_2O_5. A linear relationship was found between the content of Sb and I_{rel}, irrespective of the valence state of antimony. Therefore, I_{rel} can be used as a calibration curve for analysis of antimony content in lead dioxide films.

In corrosion films, not only PbO_2 but also $PbSO_4$ may co-exist. It is desirable, therefore, to examine the applicability of the calibration curve obtained to mixed phases of PbO_2 and $PbSO_4$. Results obtained for pressed mixtures of 80 wt% $PbSO_4$ and 20 wt% PbO_2 containing various amounts of Sb_2O_3 are also plotted in the figure (closed circles), and it was found that almost the same relationship as observed for PbO_2 discs holds. These results show that the content of antimony in the corrosion films can be determined by measuring I_{rel}.

3.2. *Sputter rate of Pb, α-PbO_2 and β-PbO_2*

If the current efficiency for deposition of Pb [14] and β-PbO_2 [15, 16] is assumed to be 100%, and if the deposited lead film is assumed to be non-porous [14], then it is possible to estimate the film thickness, d, from the quantity of electricity used in the deposition. When the film is sputtered out by an Ar^+ beam to the depth corresponding to the film thickness, the signal intensity of PbO_2^- falls sharply, and the time when the film is sputtered out, t, can be determined. The average sputter rates, which are determined as values of d/t are given in Table 1.

As shown in Table 1, the sputter rate of the electrodeposited Pb was larger than that of the electrodeposited PbO_2. The mass sputtered per unit area per unit time (ng s^{-1} cm^{-2}) is also given in this table. This is based on the assumption that the porosity of the electrodeposited film was zero. Since oxides resist sputtering to a significant extent compared with the corresponding metals [17], it is thought that the difference in the sputter rates between Pb and PbO_2 is reasonable.

3.3. *In-depth analysis of antimony in the corrosion film formed by means of multi-triangular voltammetry*

For preparation of samples, the lead–antimony electrode was anodized in 5 M H_2SO_4 using a potential sweep method. The potential was scanned 50 times at 1 mV s^{-1} between 0·90 V and 1·65 V, and then held at 1·60 V for 30 min (sample 1), 1·38 V for 30 min (sample 2) or 1·12 V for 15 min (sample 3). At the potential selected, the following reactions were believed to have taken place and were confirmed by X-ray diffraction analysis on the prepared samples: oxygen evolution accompanied by complete oxidation of the film to β-PbO_2 for sample 1, complete oxidation to β-PbO_2 for sample 2 and reduction of β-PbO_2 to $PbSO_4$ for sample 3. Each sample was rinsed with de-ionized water for a few seconds and then dried under reduced pressure (in a few torr).

Fig. 3 shows typical signal intensity profiles of SbO_2^-, O^- and PbO_2^- as a function of sputtering time for sample 1. Fig. 4 gives I_{rel} as a function of the sputtering time for this sample together with the results for the other two kinds of samples. It is noticed that I_{rel} gradually increased with the sputtering time, that is, with an increase in the

Table 1. Sputter rate of samples formed by electroplating on Pt

Sample	Preparation condition of samples			Sputter rate	
	Current density ($mA\ cm^{-2}$)	Charge passed (C)	Film thickness (μm)	($nm\ s^{-1}$)	($ng\ s^{-1}\ cm^{-2}$)
Pb	10	4·2	5·8	3·8	43
	5	2·6	5·8	3·7	42
α-PbO_2	1	0·57	1·19	0·90	8·4
	0·5	0·49	1·19	1·01	9·5
β-PbO_2	2	1·15	2·38	0·95	8·9
	1	1·15	2·38	1·05	9·8
	0·5	0·58	1·19	1·23	11·5

depth of the corrosion film. The solid lines in the figure, the ends of which were equal to the sputtering time giving the maximum signal intensity of SbO_2^-, $I_{SbO_2^-}$, as shown in Fig. 3, are believed for the following reasons to correspond to the period which gives information on the corrosion films, although beyond that point monotonic increases in I_{rel} were still noticed with sputtering time. Firstly, it was found by microscopic observation during the sputtering that the substratum alloy surface appeared almost at the same time when $I_{SbO_2^-}$ reached its maximum. Secondly, the signal intensity of PbO_2^-, $I_{PbO_2^-}$, was found to depend on the partial pressure of oxygen over the lead–antimony alloy, as Fig. 5 shows. In the sputtering process for the corrosion film, neutral oxygen molecules as well as charged species must be produced from the oxide surface [18, 19]. The maximum oxygen pressure over the sample surface will be attained when the Ar^+ beam reaches the substratum face, because the surface area of the crater in the corrosion film produced by sputtering is the largest at this point. Therefore at this stage the maximum $I_{SbO_2^-}$ will be obtained.

I_{rel} was converted into antimony content by using the calibration curve shown in Fig. 2. The antimony content in the film at the film–substratum interface, was almost twice the antimony content in the substratum alloy, 8·81 at%. This result may indicate that dissolved antimony is accumulated in a corrosion film–substratum interface region [1].

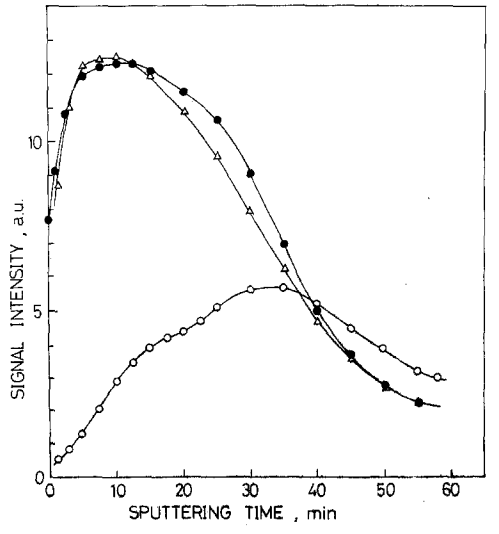

Fig. 3. In-depth profiles of $^{121}SbO_2^-$(○), $^{208}PbO_2^-$(△) and $^{16}O^-$(●) in a corrosion film on the Pb–Sb alloy.

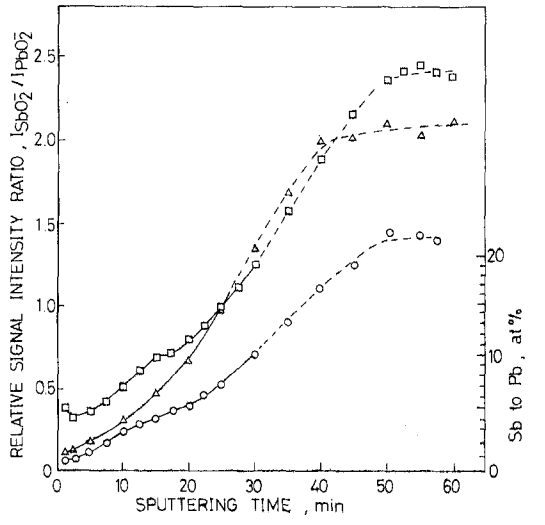

Fig. 4. I_{rel} as a function of sputtering time for samples prepared at different final polarization potentials: ○, 1·60 V; △, 1·38 V; □, 1·12 V. The solid lines show the regions of the corrosion layer.

If the solid lines in Fig. 4 represent the distribution profiles of antimony in the sample films, then we have to explain why the increasing trend in I_{rel} still continues after the beam reached the substratum alloy. For this purpose, we require a knowledge of the morphology of the corrosion film. Presumably the corrosion film will not have the same thickness throughout the analysing position. It has pores in it, and consists of aggregated particles of lead dioxide and sulphate [20, 21]. Furthermore, the substratum surface was not completely smooth. Therefore, it will be expected that when the Ar^+ beam reached the top of the substratum, some part of the film still remains on the substratum. Further continuation of sputtering will then sputter the remaining film and the substratum. It can be seen in Fig. 5 that $I_{SbO_2^-}$ is much higher than $I_{PbO_2^-}$ when the substratum alloy is sputtered. Therefore, the contribution of the secondary ions from the substratum alloy must become dominant when the sputtering proceeds from the top of the substratum to its interior. When the corrosion film is completely sputtered out, eventually no change will occur in I_{rel}.

These arguments closely relate also to resolution of the primary ion beam of IMA. The information on the beam resolution was obtained from the in-depth analysis of O^- and Ta^+ for an anodic film on tantalum. The in-depth profiles of O^- are presented in Fig. 6. By comparing the time giving a gradual signal drop, t_1, to that required for sputtering out

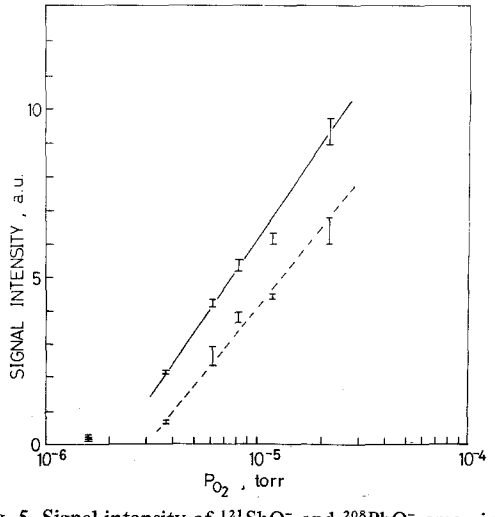

Fig. 5. Signal intensity of $^{121}SbO_2^-$ and $^{208}PbO_2^-$ emerging from the Pb–Sb alloy (4·92 wt%) as a function of oxygen pressure over the sample surface. —— SbO_2^- (× 1); - - - - PbO_2^- (× 10).

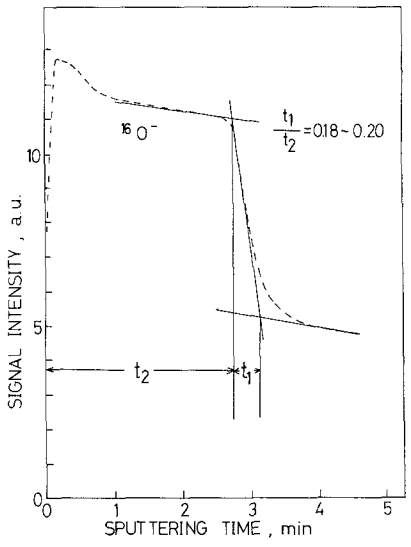

Fig. 6. Intensity profile of the secondary ion $^{16}O^-$ as a function of the depth of an anodic oxide film on tantalum (~ 50 nm thick).

the film, t_2, it can be seen that the beam resolution is as good as that usually utilized in the in-depth analysis.

The results presented in Fig. 4 show that the antimony content of the film decreased monotonically from the interior to the outer surface, independent of the final polarization potential chosen in the preparation of samples. Judging from the results on the sputter rates shown in Table 1, the thickness of the samples was around 1·8 μm. According to a model proposed by Dawson *et al.* for antimony transference during charge–discharge cycles [4], a large part of the dissolved antimony adsorbs on PbO_2, and the adsorbed antimony is released into the electrolyte during the discharge. If the distribution profiles of antimony reflect such an antimony transference, then the profile should differ greatly between samples 1 and 3. However, the results did not satisfy this expectation. The samples were, however, washed before measurements of SIMS. Washing for only a few seconds will not remove completely the electrolyte held in the pores of the corrosion film, so that antimony dissolved in this portion of electrolyte also contributes to the distribution profiles obtained.

In order to test whether this view is valid, samples were washed in an ultra-sonic bath for a fixed period of time before being mounted on a sample holder for the secondary ion mass spec-

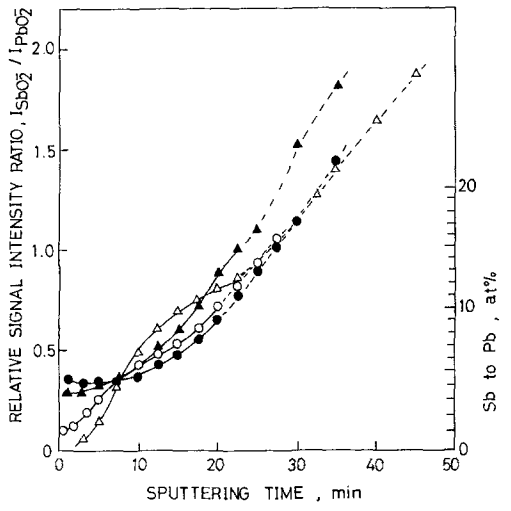

Fig. 7. Effect of washing in an ultra-sonic bath on distribution profiles of antimony in the film. The sample was prepared in the same manner as that in Fig. 3. ○, 6 min in H_2O; △, 6 min in 5 M H_2SO_4; ●, 60 min in H_2O; ▲, 60 min in 5 M H_2SO_4.

trometry. The results obtained on these samples (Fig. 7), however, show that the washing procedure does not influence the distribution profiles. Therefore, it is concluded that the corrosion films prepared by the potential sweep polarization at 1 mV s^{-1} in the potential range between 0·90 V and 1·65 V contained dissolved antimony which was tightly fixed to the corrosion film. This conclusion may be at least partly explained by the theory of Ritchie *et al.* [22] that dissolved Sb^{5+} ions might occupy vacant Pb^{4+} octahedral sites in the PbO_2 lattice and also lead to formation of lead meta-antimonate [23].

Acknowledgements

The authors thank the Yuasa Battery Co. Ltd for supplying the lead antimony alloy and to the International Lead Zinc Research Organisation, Inc. for financial support of this study.

References

[1] J. Burbank, *J. Electrochem. Soc.* **104** (1957) 693.
[2] T. F. Sharpe, *ibid* **124** (1977) 168.
[3] J. L. Dawson, J. Wilkinson and M. I. Gillibrand, *J. Inorg. Nucl. Chem.* **32** (1970) 501.
[4] J. L. Dawson, M. I. Gillibrand and J. Wilkinson, *Power Sources* **3** (1970) 1.
[5] H. W. Werner and H. A. M. de Grefte, *Vac. Tech.* **17** (1968) 37.
[6] A. Benninghoven, *Z. Phys.* **230** (1970) 403.
[7] C. A. Evans and J. P. Pemsler, *Analyt. Chem.* **42** (1970) 1060.
[8] J. M. Morabito and R. K. Lewis, *ibid* **45** (1973) 869.
[9] F. Arifuku, C. Iwakura, H. Yoneyama and H. Tamura, *Denki Kagaku* **46** (1978) 19.
[10] R. E. Pawel, J. P. Pemsler and C. A. Evans, *J. Electrochem. Soc.* **119** (1972) 24.
[11] H. Tamura, S. Yamamoto and T. Kondo, *Shinku* **14** (1971) 42.
[12] F. C. Mathers, 'Metal Finishing Guidebook', Metals and Plastics Publications Inc., New Jersy (1963) p. 332.
[13] S. Ikari, S. Yoshizawa and S. Okano, *Denki Kagaku* **27** (1959) 552.
[14] A. K. Graham, 'Electroplating Engineering Handbook', 3rd edition, Reinhold Publishing Company, New York (1971) p. 246.
[15] W. Mindt, *J. Electrochem. Soc.* **116** (1969) 1076.
[16] L. W. Higley, W. M. Dressel and E. R. Cole, Report RI 8111 (1976) Bureau of Mines, Washington DC, USA.
[17] R. Kelly and N. Q. Lam, 'Ion Surface Interaction-Sputtering and Related Phenomena', Gordon and Breach Sci. Publishers, London, New York, Paris, (1973) p. 37.
[18] C. A. Andersen, *Internat. J. Mass Spectrometry Ion Phys.* **2** (1969) 61.
[19] *Idem, ibid* **3** (1970) 412.
[20] J. J. Lander, *J. Electrochem. Soc.* **103** (1956) 1.
[21] D. Pavlov and N. Iordanov, *ibid* **117** (1970) 1103.
[22] E. J. Ritchie and J. Burbank, *ibid* **117** (1970) 299.
[23] D. E. Swets, *ibid* **120** (1973) 925.